Fast and Cyclic Shearing of Cemented Sand in Earthquake-Induced Landslide

Motoyuki Suzuki
Yamaguchi University, Japan

Takeo Umezaki
Shinshu University, Japan

Hiroshi Takahara
Penta-Ocean Construction Co., Ltd., Japan

SUMMARY:
In recent earthquakes, lots of landslides occurred in natural slopes composed of weakly cemented sands during or immediately after earthquake. The slope failure may be resultant from any loss of cementation formed between sand particles. Therefore, it is important to clarify strength property of natural cemented sand on a slip surface subjected to dynamic shearing. In this study fast and cyclic shear characteristics of cemented sands were considered based on results of ring shear test. In laboratory, artificial cementation property was reproduced by adding a cement agent to sand. A series of dynamic ring shear tests was carried out on both of non-cemented and cemented sands. Consequently, it was shown that the importance of shear strength of cemented sand was recognized when we correctly assess the stability of the slope during or after an earthquake.

Keywords: Earthquake, Landslide, Cementation, Ring shear test

1. INTRODUCTION

Mitigation of natural disasters is becoming an increasingly important and urgent matter in today's world. In particular, the potential for earthquake-induced landslides is a serious problem in hilly and mountainous regions like Japan. Therefore, it is very important to predict and control the behavior of earthquake-induced landslides in order to prevent the loss of human lives and property.

Landslides occur in natural slopes during or immediately after earthquake. The 2004 Niigata Prefecture Chuetsu earthquake triggered numerous landslides in natural slopes composed of sedimentary rocks such as sandstone, mudstone and other weakly cemented soils (see Fig.1). According to many case histories, it was shown that an earthquake-induced landslide occurred either on a slip surface in sandstone or on a bedding plane between sandstone and mudstone. Such soils possess natural cementation property due to diagenesis for a long period.

Such collapse may be due to any loss of cementation formed between sand particles. Therefore, it is important to analyse seismic slope stability based on the shear strength of natural cemented sand on

Figure 1. Tufaceous sandstone on slip surface at Yokowatashi in Nagaoka

the slip surface subjected to rapid and dynamic loading. However, the dynamic behavior and strength characteristics of cemented sand have not yet been clarified.

The aim of this study was to clarify cyclic shear behavior of cemented sand, and to develop a method for evaluating its seismic slope stability. We developed a cyclic loading ring shear test apparatus under a constant volume condition. Monotonic fast and cyclic shearing tests were carried out on both non-cemented and cemented sands using this apparatus. Laboratory-simulated cementation was artificially reproduced by adding a cementing agent to Toyoura sand. This paper describes the behavior and shear strength of cemented sand subjected to dynamic loading and the rate effect on the shear strength.

2. FAST SHEARING OF SANDS IN RING SHEAR TEST

2.1. Purpose of Test

The purpose of our test was to investigate the rate effect on the steady-state strength of cemented and non-cemented sands. A series of ring shear tests was carried out using different shear displacement rates on multiple specimens. The soil samples used were two kinds of sands collected at landslides from the Niigata Prefecture Chuetsu earthquake, namely, Terano and Higashi-Takazawa A. In addition, Toyoura standard sand was used for testing cemented sand. The shear displacement rate was changed within the range of 0.1 and 20 mm/min.

2.2. Physical Properties of Soil Samples Used

Sands were collected at croplines at the bottom of landslide slopes and labeled "*Terano*" or "*Higashi-Takezawa A*" accordingly. The samples to be used for the shear test were passed through an 0.85-mm sieve. The grading curves of samples are shown in Figure 2.

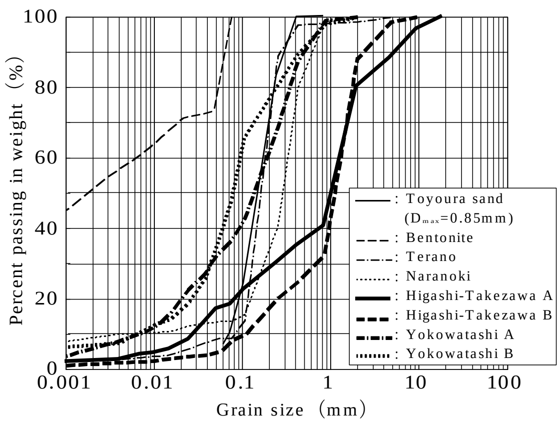

Figure 2. Grading curves of soil samples used

As above mentioned, Toyoura standard sand was also used in this study, mixed with a small amount of bentonite. The physical property of the bentonite used was ρ_s=2.716g/cm^3, w_L=479% and w_P=37%. The cemented sand was mixed at a weight ratio of Toyoura sand: bentonite: cement: distilled water of 73.7%: 5.6%: 2.0%: 18.7%. The cement content with respect to the soils was 2.5 %. The cemented sample was cured in a mold for three days. After that, a specimen was cut from the sample. The non-cemented sample was mixed at a weight ratio of Toyoura sand: bentonite: distilled water =75.6%: 5.7%: 18.7%. The sample was pre-consolidated until the end of the primary consolidation elapsed. After the consolidation, a specimen was cut from this sample. Reproduced samples were labeled "*Cemented sand*" and "*Non-cemented sand*", respectively. The ring shear test was conducted on both samples. The physical properties of the samples are listed in Table 1.

Table 1. Physical properties of sands used in this study

Soil sample	Maximum grain size, D_{max} (mm)	Soil particle density, ρ_s (g/cm^3)	Uniformity coefficient, U_C	Coefficient of curvature, U_C'
Terano	0.85	2.616	2.1	0.9
Higashi-Takezawa A	0.85	2.588	2.1	1.5
Toyoura sand	0.85	2.639	2.1	1.0

2.3. Test Apparatus and Procedure

Figure 3 shows a view of the test apparatus. The ring-shaped specimens had inner diameters of 6 cm, outer diameters of 10 cm, and a wall thickness of 2 cm. The specimens were sheared at a level of 1 cm from the base plate. During testing, shear stress, normal stress, frictional force and normal displacement were all measured and automatically recorded. The frictional force along the perimeter of the rings, which is generated by vertical displacement of the specimen, was measured by a load cell. In this test, the net normal stress acting on the shear surface was calculated based on the measurement of the frictional force.

Figure 3. Ring shear test apparatus used

The specimen was carefully compacted with three layers using a tamper in order to ensure that the initial dry density of the specimen could be established uniformly. The upper surface of the specimen was finished flat. After that, the specimen was normally consolidated by consolidation stress, σ_C, for one hour. The value of σ_C was varied within the range of 294 to 490 kPa, since the depth of the slip surface in both landslides was equivalent to about 30 m. After consolidation, the specimen was sheared under a constant total normal stress, σ_N, until shear displacement, δ, became a value sufficiently large to reach a steady state. Here δ is defined as an intermediate circular arc between the inner and outer rings. Before the shearing, the minimum gap between the rings was opened in order to remove the friction between the rings, and to avoid the outflow of the sample from the shear surface.

2.4. Results and Discussions

Determination of the strength parameter for dense dried sand and its rate effect are discussed in this section. Figures 4 (a) and (b) show test results of Terano and Higash-Takezawa A. The relationships between the peak and steady-state strengths, τ_p, τ_{ss}, and the normal stress with different shear displacement rates are shown in these figures. The steady state of sand was defined as an ultimate state in which the stress ratio, τ/σ_N, of sand did not change as the shearing proceeded. The strength parameters at the peak and steady states as shown in these figures were determined by fitting to the measurement of the relationship among the peak strength, the steady-state strength, and the normal stress using the least square method. It can be seen from this figure that the apparent cohesion in all cases was almost zero, because of dried sand. On the other hand, there can be seen a slight change in the gradient of the peak and steady-state strength lines.

Next, the rate effect observed in dense sands was considered. Figures 5 (a) and (b) show the relationships between the internal friction angle at peak and steady states, and the shear displacement angle rate for Terano and Higashi-Takezawa A. The peak value for Terano slightly increased or decreased within the range of 0.1 to 20 mm/min, whereas the steady-state value remained almost constant in the same range. On the other hand, the internal frictional angles at both states for Higashi-Takezawa A remained almost constant in the same range. At least, the internal friction angle at the steady state was not changed by any change in the shearing speed. This finding is consistent with that of dense Toyoura sand. However, these sands were well graded as compared that of Toyoura sand. It was shown that the internal frictional angles at the peak and steady states were not affected by any change in the shearing speed.

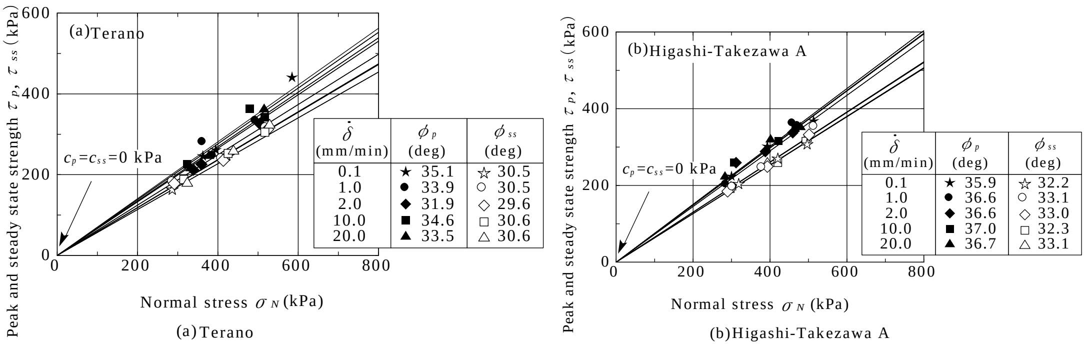

Figure 4. Peak and steady-state strength lines of (a) Terano and (b) Higashi-Takezawa A

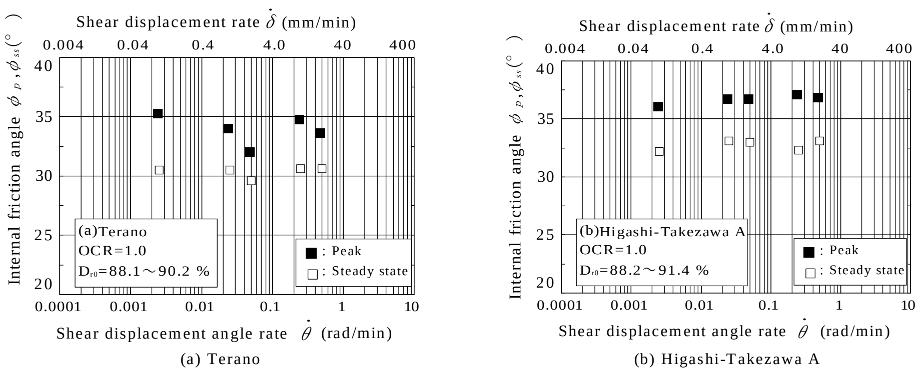

Figure 5. Relationship between internal frictional angle in peak and steady states and shear displacement rate

Figure 6 shows the relationship between shear stress and normal stress on the shear surface for cemented and non-cemented sands. In this test, the normal stress was gradually decreased in the steady state. The internal friction angles in the steady state of both sands were at the same level as that of Toyoura sand. The apparent cohesion of the cemented sand was c_{ss}=18.5kPa, the large value of which may be due to development of the cementation.

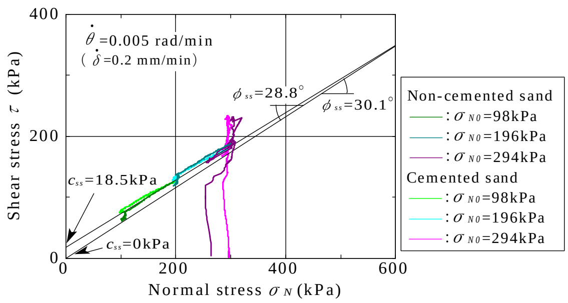

Figure 6. Stress paths and strength lines of cemented and non-cemented sands

Figure 7 shows the relationship between the stress ratio in steady state and the shear displacement rate in a logarithmic scale for non-cemented and cemented sands. These data were obtained by shear testing using a single specimen as shown in Fig.6. The stress ratio for non-cemented sand was almost constant despite the change of the shear displacement rate. On the other hand, the stress ratio for cemented sand decreased with increases of the shear displacement rate and then became close to that for non-cemented sand. It was suggested that the cementation property of the shearing zone in the cemented sand was gradually damaged by shearing and eventually disappeared.

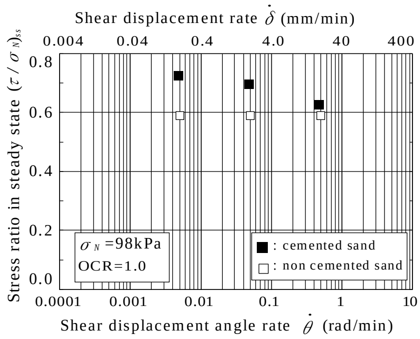

Figure 7. Relationship between steady-state stress ratio and shear displacement rate of cemented and non-cemented sands

Figure 8 shows the relationship between the residual or steady-state strength of various soils and shear displacement rate. A lot of data quoted from previous studies were plotted in this figure. Sandy soils generally exhibit higher shear strength than clayey soils. However, the residual strengths of some clays are higher than those of sands. It can be seen from this figure that clay exhibited significant rate effect on its residual state strength, whereas sand did not exhibit any rate effect on its steady state strength. In some clays, the residual stress ratio increased, decreased, or remained constant according to the change of the shear displacement rate. This tendency appeared with the change of effective normal stress on the shear surface owing to the generation of excess pore water pressure. In the case of dried sands, there did not exist excess pore water pressure as in clay. In the range of high normal stress, the amount of dilation was small, so that the rate effect was negligible.

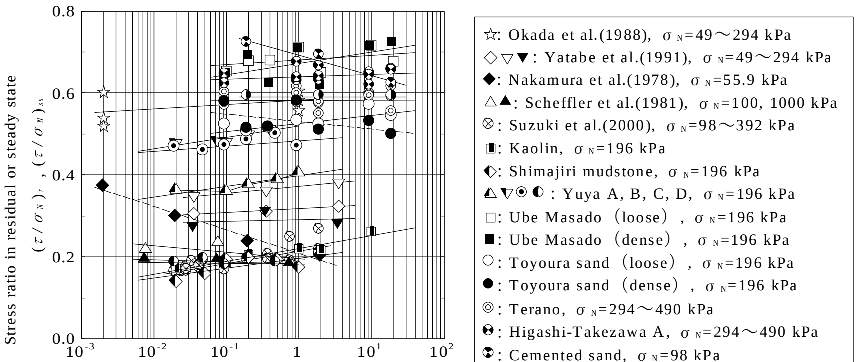

Figure 8. Effect of shear displacement rate on residual or steady-state shear strength of various soils

Figure 9 shows grading curves of Terano before and after the shearing. This figure shows that the fine content of the sample increased after shearing. According to Lupini et al. (1981), the transitional shearing zone contained sliding, and turbulent shearing modes occurred within the range of the clay fraction, F_{clay}=23~43%. The steady state line of the sand was slightly affected by the shearing rate as shown in Fig.4 (a). Crushable soil seems to move toward each steady state line while its fine content increases during shearing.

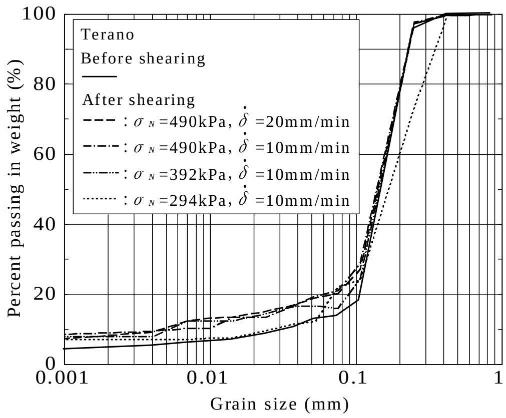

Figure 9. Change of grading curves of Terano before and after shearing

3. CYCLIC SHEARING OF SANDS IN RING SHEAR TEST

3.1. Purpose of Test

In the Niigata Prefecture Chuetsu earthquake of 2004, a number of landslides occurred. In particular, it was found that natural slope consisting of sandstone was vulnerable to seismic motion. It is considered that undisturbed sand loses its cementation property by cyclic shearing, and reduces its intrinsic strength, which then led to large-scale collapse. Many researchers are researching the dynamic shear strength of clay and silt. However, the cyclic shear strength and shear behavior of sandy soil having low cementation has not been clarified. Therefore, the purpose of this test was to elucidate the cyclic shear strength of minimally cemented soil. By adding the cementing agent to the soil sample, cemented sand was constituted as a model of natural cementation. The shear behavior of weakly cemented sand was examined using the constant volume cyclic loading ring shear test.

3.2. Specimen Preparation and Physical Properties of Sample

As above mentioned, the samples used in this study were artificially reproduced by mixing Toyoura standard sand with a small amount of bentonite and cement. Cemented sand was cured for three days under constant temperature. The soil hardness value of the specimen reached the field value equivalent of 26.3 mm during two or three days of curing. After the curing, the specimen was cut 6 cm in inner diameter, 10 cm in outer diameter, and 2 cm in height. Cyclic ring shear tests were carried out on three samples; Toyoura sand, non-cemented and cemented sands. The initial void ratio of the specimen was e_0=0.641~0.645 for Toyoura sand, e_0=0.683~0.954 for non-cemented sand, and e_0=0.724~0.776 for cemented sand.

3.3. Test Apparatus and Procedure

Figure 10 shows the constant volume cyclic loading ring shear test apparatus. This apparatus consisted of a cyclic ring shear test apparatus and pneumatic servo controller, two bellofram cylinders, constant volume-control device, dynamic strain data logger, and personal computer for data recording. A specimen was placed in the ring shear box, and consolidated by applying consolidated pressure σ_N =98~294kPa. After the consolidation, the specimen underwent cyclic shearing. During the testing, shear stress, τ, normal stress, σ_N, horizontal displacement, δ, frictional force and vertical displacement, v, were all measured and automatically recorded.

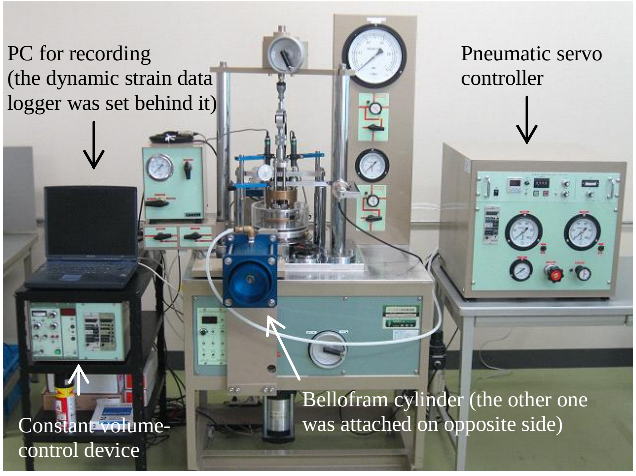

Figure 10. Cyclic ring shear test system

3.4. Results and Discussions

Figure 11 shows the time histories of σ_N, τ, v and δ for non-cemented and cemented sands. With the progress of the shear, σ_N was reduced so as to maintain a constant volume condition, which eventually became constant. The amplitude of τ was gradually increased, and finally became almost constant. On the other hand, δ increased gradually. In addition, v was controlled to be a small and constant volume. However the vertical displacement was not always constant during cyclic shearing, since the leakage of soil sample from the gap between the rings was observed. In this study, the waveform of the applied shear stress during cyclic shearing is like a sine wave. However, the measured waveform was more or less different from the applied one. Therefore, the measured curve was replaced by a τ~t curve with a constant amplitude equivalent to that with irregular amplitude. The determination of the cyclic shear stress ratio and the number of cycles at failure was carried out based on the replaced τ~t curve. In typical shear behavior, the normal stress became nearly zero around δ= 2~3 mm. Also, the width of shear zone mainly depends on the mean grain diameter of sample. When the shear displacement was at 2 mm, the equivalent shear strain attained over 100 %. Therefore, the cyclic shear failure was defined as the point at which δ had reached -2 mm.

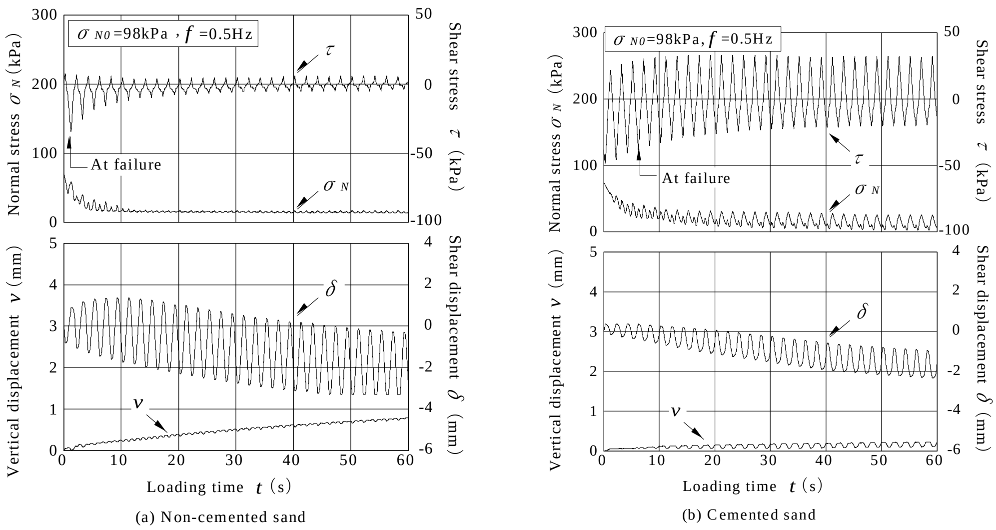

Figure 11. Time history of cyclic behavior of (a) non-cemented and (b) cemented sands, respectively

Figure 12 shows the relationship between σ_N and τ of Toyoura sand, non-cemented and cemented sands, respectively. In addition, this figure shows the steady-state strength line (SSSL) obtained from another ring shear test under constant pressure. The stress paths of Toyoura sand and non-cemented sand reached their steady-state strength line. The stress path of cemented sand reached its steady-state strength line. Each stress paths obtained by the cyclic shearing reached the SSSL of the material. However, there was no clear sign of liquefaction just for these results. This suggested that cemented sand can collapse before loss of cementation. After the cementation property of cemented sand layer was lost by earthquake, general shear failure might occur in the slope.

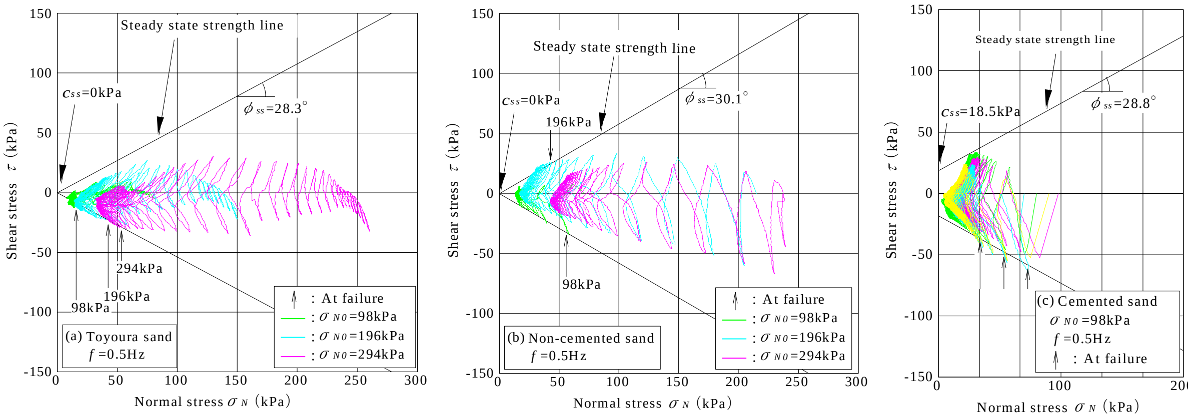

Figure 12. Stress paths and steady state strength lines of (a) Toyoura sand, (b) non-cemented sand and (c) cemented sands during cyclic shearing, respectively

Figure 13 shows the relationship between the shear stress ratio, τ/σ_{N0}, and the number of cycles at failure point, N_f. Here, σ_{N0} is the initial normal stress in the process of cyclic shearing. This figure shows the results of non-cemented and cemented sands. In both sands, τ/σ_{N0} becomes larger when N_f becomes smaller. There seems to be a correlation between τ/σ_{N0} and N_f. The τ/σ_{N0} and N_f curve of cemented sand may move upward when the amount of cementing agent was increased. In the τ/σ_{N0} ~N_f curve, the effect by cementation was confirmed.

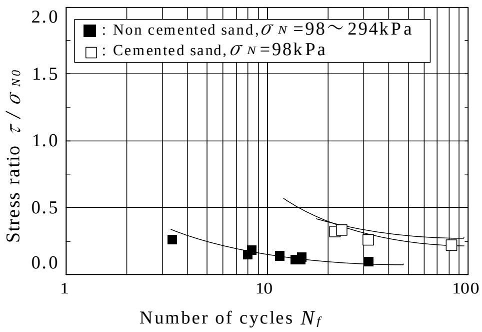

Figure13. Relationship between stress ratio and number of cycles for non-cemented and cemented sands

4. CONCLUSIONS

The following conclusions can be derived from the results and the discussion. 1) The steady-state strength of non-cemented sand was hardly affected by changes in the shear displacement rate within the range of 0.1 to 20 mm/min. 2) The fine content of sand specimens with high dry density increased owing to particle crushing during fast shearing. 3) As the shear displacement rate increased at the steady state, the shear stress of cemented sand gradually decreased. Finally, the shear stress mobilized on the slip surface reached the steady-state strength of non-cemented sand. 4) At the end of cyclic loading, the stress path of cemented sand reached its steady-state strength line, which could be determined by a consolidated drained ring shear test. Simultaneously, the cumulative displacement rapidly increased. 5) The seismic stability of a slope consisting of naturally cemented soil can be evaluated based on its steady state strength parameter and the effective normal stress at failure on the slip surface.

AKCNOWLEDGEMENT

The authors are grateful to Mr. Kimihiro Fujii and Mr. Sho Fujii for their experimental assistance. This work was supported by KAKENHI (20560464). We express sincere thanks to them.

REFERENCES

Lupini, J.F., Skinner, A.E. and Vaughan, P.R. (1981). The drained residual strength of cohesive soils. *Géotechnique*. **31:2**, 181-213.

Nakamura, H. and Shimizu, K. (1978). Soil tests for the determination of shear strength along the sliding surface. *Landslide*. **15:2**, 25-32 (*in Japanese*).

Okada, F. and So, E. (1988). Relation between residual strength and microstructure. *Proc. of the 23th Japan National Conference on Geotechnical Engineering*. 227-228 (*in Japanese*).

Scheffler, H. and Ullrich, W. (1981). Determination of drained shear strength of cohesive soils. *Proc. of 10th I.C.S.M.F.E.* **10:** 775-778.

Suzuki, M., Umezaki, T., Kawakami, H. and Yamamoto, T. (2000). Residual strength of soil by direct shear test. *Journal of Geotechnical Engineering*. **645:III-50**, 37-50 (*in Japanese*).

Yatabe, R., Yagi, N. and Enoki, M. (1991). Ring shear characteristics of clays in fractured-zone-landslide. *Journal of Geotechnical Engineering*. **436:III-16**, 93-101 (*in Japanese*).